Fibers and Polymers 2013, Vol.14, No.11, 1877-1885 DOI 10.1007/s12221-013-1877-6

Impact Properties of Glass-fiber/Polypropylene Composites: The Influence of Fiber Loading, Specimen Geometry and Test Temperature

Normasmira A. Rahman, Aziz Hassan*, R. Yahya, and R. A. Lafia-Araga

Polymer and Composite Materials Research Laboratory, Department of Chemistry, University of Malaya, 50603 Kuala Lumpur, Malaysia

(Received October 16, 2012; Revised May 9, 2013; Accepted May 15, 2013)

Abstract: Glass fiber reinforced polypropylene composites were compounded with a twin-screw extruder and injection molded. Fiber length distribution study showed that more fiber degradation occurred during processing of the composites with higher fiber loading. Dynamic mechanical analysis carried out showed that magnitudes of storage and loss modulus of composites are improves with the presence of the glass fiber in the system. The incorporation of fibers into the composites has slightly shifted the glass transition temperature to lower values. On the other hand, the presence of the glass fiber reduces the magnitude of tan δ at α-transition dramatically due to the strengthening effect by the fibers. From impact test, it was found that increment in glass fiber loading leads to an increase in peak load, critical strain energy release rate and critical stress intensity factor indicating the improvement in the material toughness. However, there was no significant change observed in fracture energy. With respect to increasing in specimen geometry, despite an improvement in peak load and fracture energy of the impact specimen, the critical strain energy release rate and critical stress intensity factor values were decreased. On the other hand, increase in test temperature resulted in reduction of peak load and critical stress intensity factor due to increment in material ductility, whereby fracture energy and critical strain energy release rate improved.

Keywords: Glass fiber composite, Dynamic mechanical properties, Impact properties, Specimen geometry, Temperature

Introduction

It has been demonstrated that polypropylene (PP) filled with glass fiber (GF), carbon fiber, calcium carbonate, clay and other fillers can successfully bridge the gap in performance between neat commodity plastics, engineering resins and short-fiber reinforced thermoplastics. These materials are being used increasingly due to their superior strength, light weight and adaptable design, where the ability to tailor their mechanical properties is by the choice of fiber, fiber direction and matrix. Moreover, toughness of polymeric materials is very often the decisive parameter used in material selection for a wide variety of applications such as automotive, home appliances, construction, utilities, and sporting goods [1]. However, their behavior in impact properties determination is very complex due to a large number of factors that govern their response [2]. Charpy impact testing is a cheap yet reliable method to study the fracture behavior and impact strength of materials [3]. It is commonly required for construction codes, especially for fracture-critical structures such as bridges and pressure vessels. However, the method is highly sensitive to changes in test parameters such as impact velocity, specimen geometry, shape and size of impactor tup, clamping mode, matrix properties, reinforcement geometry and energy supplied, etc [4-6]. Without uniformity of test results, the impact tests are almost meaningless as comparisons cannot be made. Therefore, it is vital to study the factors affecting the impact results scatter in order to have a better understanding of the test methods applied [7].

*Corresponding author: ahassan@um.edu.my

In contrast to metals which absorb energy in elastic-plastic deformation, fiber-reinforced polymer (FRP) exhibit a variety of fracture mechanisms including matrix deformation and micro-cracking, interfacial debonding, lamina splitting, delamination, fiber breakage and fiber pull-out [8]. The effect of fiber volume fraction on the impact performance of glass fiber reinforced polymer (GFRP) had been studied by various investigations with contradictory results. It was found that increased in the fiber content increased the impact resistance [9]. However, Khalid [10] found an opposite trend, which increase in the fiber content led to a reduction in the impact resistance.

The study of impact response of composites subjected to environmental conditions other than ambient is more realistic. A few studies have focused on the effect of temperature on the impact response of polymer matrix composites. The charpy impact strength of PP laminates with different lengths and concentrations of glass fiber at temperature range of $-50\,^{o}C$ to $40\,^{o}C$ had been studied by Thomason and Vlug [11]. The authors concluded that as the test temperature increased, the laminate impact strength decreased. The effect of temperature exposure and glass fiber content on the impact behavior of polyester laminates composites has been reported. It was suggested that the effect of exposure temperature and fiber volume fraction on impact strength of GFRP composite depends on the parameter controlling the mode of failure [2]. On the contrary, results from another study [10] showed the inversed behavior, where an increase in the impact resistance was found with increasing temperature.

There is inadequate data available about the phenomena behind the impact property response due to the variation in

fiber concentration, specimen dimension and temperature. Motivated by this fact, here we report the effect of the main testing parameters, namely specimen size/geometry, glass fiber loading and test temperatures on the impact properties of injection molded polypropylene composites. The morphology, fiber length distribution and dynamic mechanical properties of injection molded glass fiber reinforced PP composites were also investigated.

Experimental

Materials and Specimen Preparation

PP (Propelinas H022) was supplied by Petronas, Malaysia. The neat PP was in the form of pellets with a melt flow index of 11 g/10 min and a density of 910 kg m^{-3}. Chopped E-glass fiber, surface-treated with silane and having a density of 2,550 kg m^{-3}, diameter of 14 μm and length of 6 mm, obtained from KCC Corporation, Korea and used as the principal reinforcement.

The materials in different ratios of PP/glass fibers were physically pre-mixed and then compounded using a Brabender, KETSE 20/40 (Germany) twin screw extruder with the screw diameter and aspect ratio of 20 mm and 40, respectively. The temperature profile was set to 185-190 °C. The extruded materials were pelletized to length of about 6 mm. The dumb bell-shaped tensile and impact tests specimens, according to ASTM D-638 standard [12] and ASTM E-23 standard [3], respectively, were then injection molded using a Boy® 55M (Germany), a 55 tonne clamping force injection molding machine. The mold used for tensile and impact specimens preparation were single gated with four and eight cavities, respectively. The processing temperature was set between 175-185 °C and the mold temperature was set at 25 °C. The screw speed was maintained at 30-50 rpm. Specimens were designated according to their types and composition; for example T/G15 and I/G15 were referred as tensile and impact specimen, respectively, with 15 % fiber weight fraction (W_f) of GF.

Microstructural Characterization

The fracture surface of the various composites was examined using a JEOL Field Emission Auger Microprobe model JAMP-9500F (Japan) under scanning electron microscopy (SEM) mode to investigate the effects of glass fiber concentration and temperature on the impact fracture behavior. SEM micrographs were taken at 10 keV acceleration voltage at various magnifications. The fracture surface of tensile specimens was sputter-coated with a thin layer of gold in order to improve the sample conductivity and to avoid electrical charging during examination.

Determination of Fiber Length Distribution (FLD)

Samples from the central portion of injection-molded tensile test pieces were cut and the polymer matrix was removed by heating the composite specimen in a muffle furnace at a temperature of 700 °C for a period of about 6 hours. The extracted fibers were used in order to determine the FLD. Lengths of not less than 500 fibers were measured using image analyzer (Leco model IA-32, USA).

Determination of Dynamic Mechanical Properties

The dynamic mechanical properties of specimens were analyzed with a Dynamic Mechanical Analyzer, DMA Q800 (Thermal Analysis Instrument, USA). Test specimens were taken from the middle section of the injection molded dumb-bell tensile test bar and were subjected to a three-point bending mode with a support span of 50 mm. Measurements were conducted over a temperature range of –100 °C to 110 °C with a heating rate of 3 °C min^{-1} under a constant frequency of 1.0 Hz.

Determination of Impact Properties

Charpy impact tests were conducted using an Instron Dynatup 9210 Falling Weight Impact Tester with a V-shaped impactor tup. The tensile and impact test bars (Figure 1(a) and (b)) were notched with a V-notch at the centre of one edge to produce single edge notch (SEN) test specimen. Each batch was notched with a notch-to-depth (*a/D*) ratio of 0.2. The notch angle was set at 45 °. Details of specimen

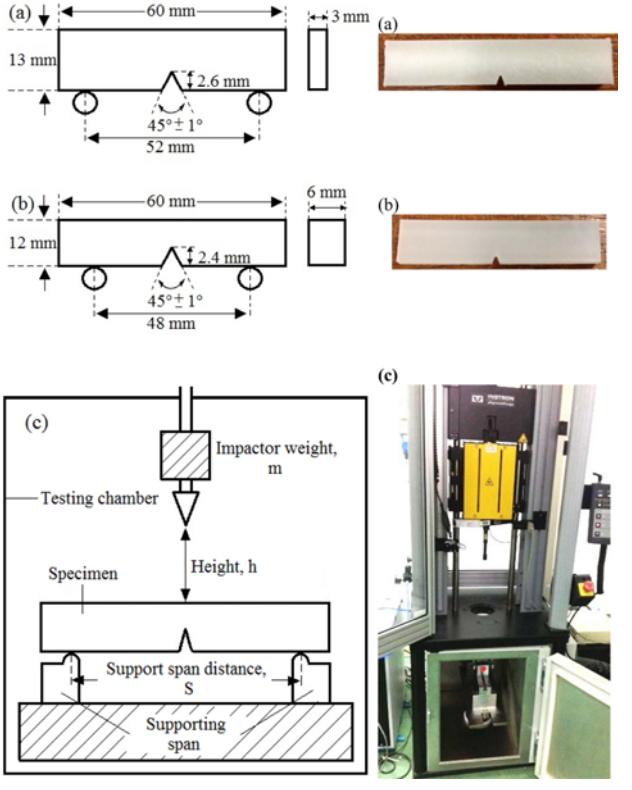

Figure 1. Specimen geometry and photographic images of (a) tensile and (b) impact specimens; and (c) specimen/testing arrangement in impact test.

arrangement and impactor setup are shown in Figure 1(c). For each batch, a minimum of 10 specimens were tested and the results presented were taken from the average of at least 7 reproducible data. The test was carried out in testing chamber at different temperatures of 25 °C, 50 °C and 75 °C, with fixed impactor velocity of 0.87 m s^{-1} and impact energy of 2.11 J.

Results and Discussion

Fiber Length Distribution (FLD)

Plots of FLD of composites extracted from the tensile test specimen are shown in Figure 2. From this figure, it can be seen that for all specimens, fiber distributions are quite normal, tailing towards the longer fiber length. The same observation was reported by Hassan *et al.* [13]. The plots in Figure 3 (cumulative FLD) also show that more fiber population with shorter length occurred in composites with higher fiber loading, whereby the composites with lower fiber loading have more fiber population with longer length. This indicates more fiber degradation has taken place during compounding and molding of composites with high fiber loading, probably due to fiber-fiber, fiber-matrix and fiber-machinery surface friction. In addition, high melt viscosity and increased tendency for high fiber contact are probably responsible for the higher fiber breakage in this category of composites [13,14].

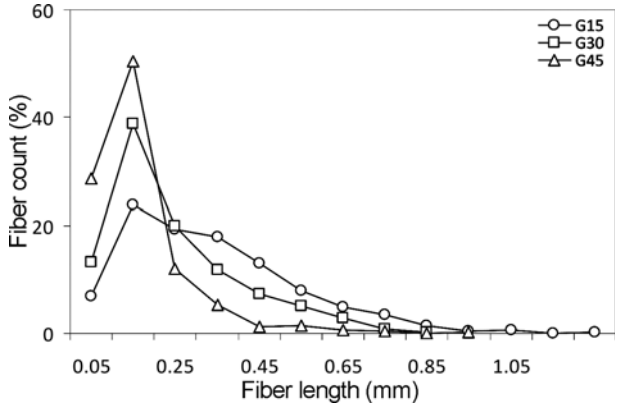

Figure 2. FLD of injection-molded glass fiber composites.

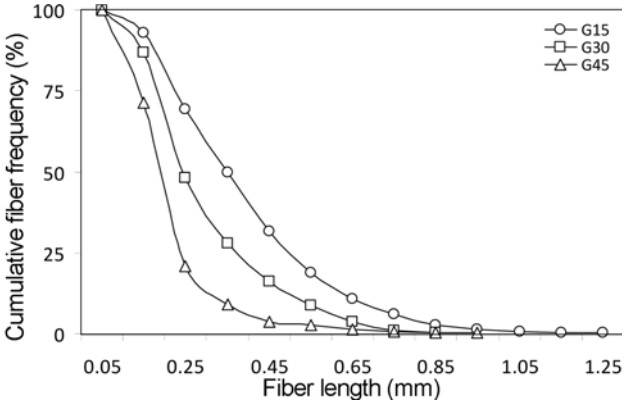

Figure 3. Cumulative fiber frequency of injection-molded glass fiber composites.

The number average fiber length ($\overline{L}_n$) that presents a measure of fiber ends density and weight average fiber length ($\overline{L}_w$) which gives a greater importance to the proportion of long fibers in the distribution were also calculated using standard equations [13,15]. Generally, $\overline{L}_n$ and $\overline{L}_w$ decrease with an increase in fiber loading. The $\overline{L}_n$ values reduced from 0.33 for G15 to 0.24 mm and 0.16 mm for G30 and G45, respectively. Furthermore, the $\overline{L}_w$ values also reduced from 0.46 for G15 to 0.35 mm and 0.24 mm for G30 and G45, respectively. These results are in agreement with earlier reports whereby more fiber degradation occurred with an increase in fiber loading [16-18].

Dynamic Mechanical Analysis (DMA)

DMA results of composite specimens are shown in Figure

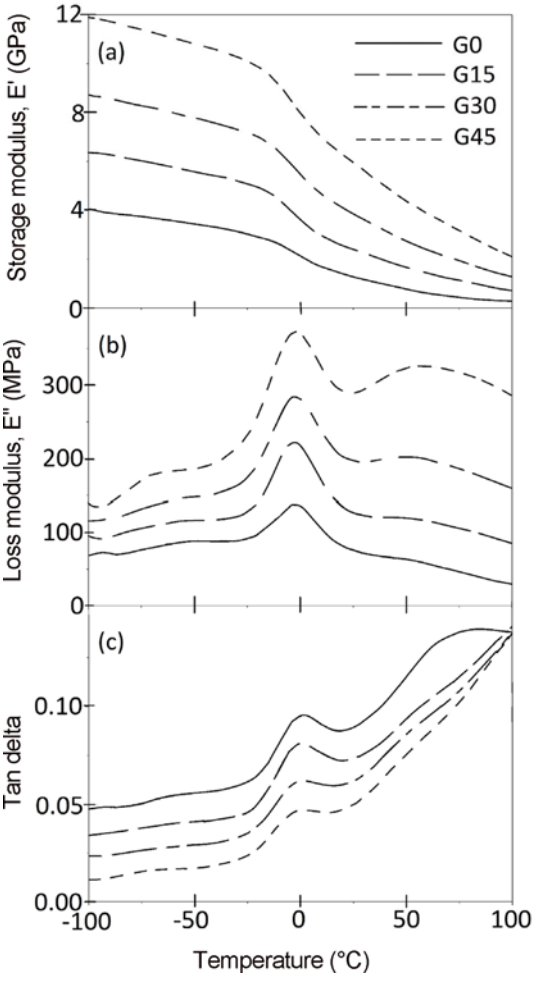

Figure 4. The DMA curves of composite specimens with different fiber loadings (Tan delta curves are shifted vertically for clarity; G0 (+0.03), G15 (+0.02), G30 (+0.01) and G45 (original position)).

4. From this figure, over a temperature range of −100 °C to 110 °C, only one major transition is detected between −25 °C to 25 °C which is related to glass transition region.

Storage Modulus (*E′*)

The storage modulus (*E′*) is closely related to the load bearing capacity of a material and is analogous to the flexural modulus measured as per ASTM D-790 standard [19,20]. Variation of *E′* as a function of temperature for composites with different glass fiber loadings is graphically presented in Figure 4(a). From this figure, a decreasing trend in the storage modulus over the whole temperature range is observed. A significant fall in *E′* is noticed in the region between −25 °C and 25 °C which is believed to correspond to the glass transition region of the matrix polymer. However, with incorporation of fiber, decrease in *E′* is being compensated by the interaction caused by the reinforcing effect of fibers in the matrix [21]. It is evident from Figure 4(a) that there is a notable increase in the modulus with incorporation of glass fibers, probably caused by increase in the stiffness of the matrix due to reinforcing effect imparted by the fibers allowing greater degree of stress transfer at the interface [22]. The storage moduli of the composites at −100 °C are increased from 4.06 GPa for PP matrix to 6.36 GPa, 8.72 GPa and 11.89 GPa for G15, G30 and G45, respectively.

Loss Modulus (*E′′*)

The loss modulus (*E″*) is defined as the amount of energy dissipated or lost as heat per cycle of sinusoidal deformation, when different systems are compared at the same strain amplitude. It is the viscous response of the material [23]. In this work, $T_{\alpha}^{E''}$ is referred to as the temperature at the maximum value of loss modulus in the α-transition region, while the $E''_{\max}$ and $E''_{25^{\circ}C}$ are the magnitude of loss modulus at $T_{\alpha}^{E''}$ and at 25 °C, respectively.

The loss modulus, *E″* curves for PP matrix and composites at different glass fiber loadings are shown in Figure 4(b). The addition of glass fibers in the PP matrix shows insignificant changes in the $T_{\alpha}^{E''}$ value, relative to the neat PP. By contrast, the $E''_{\max}$ values for the glass fiber composites are higher compared to PP matrix. An arithmetic increment of 61 %, 105 % and 168 % are observed for G15, G30 and G45, respectively. The higher modulus at $T_{\alpha}^{E''}$ is possibly due to the presence of glass fibers which reduces the flexibility of the material by introducing constraints on the segmental mobility of the polymer chains at the relaxation temperature. Moreover, broadening of the transition region is observed in all composites system, indicating segmental immobilization of matrix chain [21]. A similar trend is observed for $E''_{25^{\circ}C}$ with more prominent improvement. Geometric increment of about 68 %, 162 % and 286 % were obtained with incorporation of 15 % W_f, 30 % W_f and 45 % W_f of glass fiber, respectively, in the composites system.

Loss Tangent (tan δ)

The ratio of loss modulus to storage modulus is measured as the mechanical loss or damping factor (tan δ). The damping properties of the material give the balance between the elastic phase and viscous phase in a polymeric structure [24,25]. In the present investigation, the variation of tan δ as a function of temperature is represented in Figure 4(c). The transition region as indicated by damping maxima is usually known as α-transition. The peak at maximum value of tan δ in α-transition, T_{α}, is generally referred to as the glass transition temperature, T_g. Meanwhile, the tan $\delta_{\max}$ is refer to the magnitude of tan δ at T_g.

As shown in Figure 4(c), the incorporation of the fibers into systems has slightly shifted the T_g to lower temperatures. At higher glass fiber loading, fiber/matrix wetting problem might have occurred (poor adhesion), leading to increase in segmental mobility of the polymer chain, thus resulting in decrease in T_g [21]. In addition, the presence of the glass fiber reduces the magnitude of tan $\delta_{\max}$ values. Higher reduction for composites with higher fiber loadings is believed to be due to the strengthening effect by the fibers which limit the mobility of the polymer matrix. Tan $\delta_{\max}$ of G45 shows a maximum decrease of about 30 % compared to the PP matrix (0.067 to 0.047). In this case, the incorporation of fibers acts as barriers to the mobility of polymer chain, leading to lower degree of molecular motion and hence lower damping characteristics [26]. Another possible reason is that there is a less weight fraction of PP matrix to dissipate the vibration energy [18].

Impact Properties

Effect of Fiber Concentration and Specimen Geometry

Histogram of peak load (P) and fracture energy (W) against W_f for different specimen sizes at 25 °C are depicted in Figure 5. From the histogram, it can be observed that, generally, the P values increase with respect to increasing

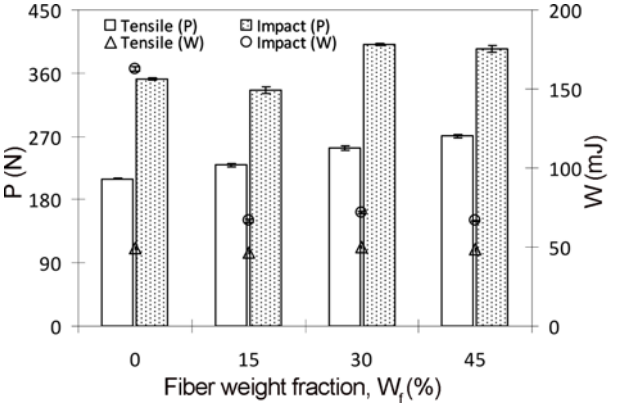

Figure 5. Peak load (P) and fracture energy (W) of composite specimens with different fiber loadings and specimen dimensions at 25 °C.

fiber content for the tensile specimens. This trend is expected as the presence of fibers tends to reduce resistance to crack initiation, therefore increasing the material brittleness, while at the same time reducing crack propagation through the matrix by forcing crack lines around the fiber ends [27]. For tensile specimen, no significant trend for W is observed with increase in GF content. However, for impact specimen, there is a sharp decrease in W (60 %) with the initial incorporation of 15 % W_f of GF loading compared with neat PP matrix (162 mJ). It is interesting to note that further addition of 30 % W_f (G30) and 45 % W_f (G45) of GF does not produce any significant effect on fracture energy value. Meanwhile, in order of increasing the testing temperature to 50 °C and 75 °C, identical trends in P and W values are observed.

It is also observed that at the same fiber content, W and P values increase with specimen size. The improvement of P and W for impact specimen could be due to the increment of about 68 % in cross section area (57.6 mm^2) relative to tensile specimen (34.3 mm^2). However, the enhancement in P and W for impact specimen is not proportional to the increment in cross section area. For example, the peak load value for G/15 increases by about 46 % from 230 N for tensile specimen to 336 N for impact specimen. Meanwhile, the equivalent fracture energy of impact specimen only increases to about 42 % compared with tensile specimen. This could be due to the higher tensile specimen thickness relative to impact specimen which results in longer path of crack propagation hence required more energy to break the specimen. Therefore, in the determination of impact properties, specimen dimension and specimen size are the controlling factors that need to be considered.

Critical strain energy release rate (G_c) is the total energy absorbed by test specimen divided by its net cross section area and is used to measure the energy necessary for crack initiation. G_c is a material parameter that when properly determined does not depend on specimen geometry. From the theory of fracture mechanics, a quantity called the critical stress intensity factor, K_c, characterizes the severity of the crack situation as affected by crack size, stress and geometry. Generally, the resistance to crack propagation or fracture toughness of the composites is characterized by measuring the G_c and K_c in three point bending (3-PB) according to ASTM E-23 standard [3]. Both parameters can be taken as a measure of interfacial strength. Linear elastic fracture mechanics (LEFM) methodologies have been used to characterize the toughness of composites and plastics in terms of G_c or K_c of the polymeric materials. It is found to be an effective way to characterize brittle polymers.

The relationship between W, G_c and specimen geometry parameter ($BD\Phi$) is given by [5]:

$$W = G_c BD\Phi \tag{1}$$

where B and D are the width and depth of the specimen, respectively. A correction factor, Φ is given by:

$$\Phi = \frac{1}{2}\left(\frac{a}{D}\right) + \frac{1}{18\pi}\left(\frac{S}{D}\right)\left(\frac{a}{D}\right)^{-1} \tag{2}$$

where a and S are notch depth (or crack length) and span of the specimens, respectively.

According to Hassan *et al.* [5], the impact measurement at notch to depth ratios (a/D) of 0.2 can be considered as the best approximation for the G_c value as obtained from the plot of W against $BD\Phi$. Therefore, due to limited specimen, for each batch, the impact tests were only conducted at a/D of 0.2. The re-arranged equation (1) was used to calculate the G_c value, i.e. $G_c=W/(BD\phi)$.

The relationship between the K_c with nominal fracture stress (σ), geometry correction factor (Y), and notch or crack length (a) is given by:

$$\sigma Y = \frac{K_c}{\sqrt{a}} \tag{3}$$

The re-arranged equation (3) was used to calculate the K_c value, i.e. $K_c=\sigma Y\sqrt{a}$. The variations of G_c and K_c as a function of glass fiber loading at 25 °C are presented in Figure 6. The G_c of T/G30 and I/G30 are 8 % higher compared to T/G15 and I/G15, respectively. This is due to the contribution of high stiffness of the glass fiber that resulted in the high strength of the composites. Thomason and Vlug [11] also reported that the impact strength obtained in their charpy test increased almost linearly with fiber concentration. This result indicates that as glass fiber is included in the composite, impact energy dissipation originated from fiber inclusion is more [28]. The main mechanisms suggested were the debonding between glass fiber and PP matrix and fiber pull-out [29,30]. The plastic deformation of the PP matrix also contributes to the impact energy absorption. In PP/GF system, the fracture energy absorption was shown to be dominated by contribution from matrix plasticity [29,31]. The matrix plastic deformation occurs either through homogeneous deformation of the matrix or from localized deformation around fiber ends. By contrast, for the composite

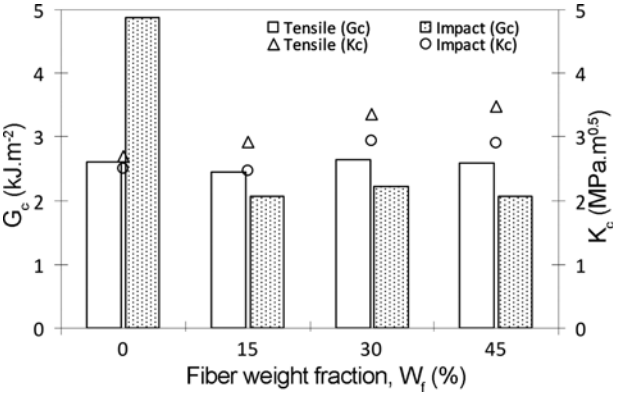

Figure 6. G_c and K_c of composite specimens with different fiber loadings and specimen dimensions at 25 °C.

with higher fiber volume fraction (T/G45 and I/G45), the G_c exhibits a decreased value, as also observed by the other researchers [28]. In the case of K_c, generally, it increases with increasing fiber content. It is evident that the fracture toughness of the glass fiber composites increases progressively with further incorporation of glass fiber.

With respect to increasing in specimen size, despite an improvement in W, the G_c value for the composites of impact specimen were decreased compared with tensile specimen. The G_c values for impact specimen were reduced by about 15 %, 16 % and 20 % for G15, G30 and G45, respectively, relative to tensile specimen with the same glass fiber content. By contrast, the G_c value for PP matrix increases by 86 % from 2.61 MPa $m^{0.5}$ (tensile specimen) to 4.87 MPa $m^{0.5}$ (impact specimen). In case of PP matrix, since the fracture is only due to matrix contribution, specimen thickness plays a very important role. Therefore, impact specimen with the thickness of 6 mm has higher G_c value relative to tensile specimen with the thickness of 3 mm. Whereas, in composites, with incorporation of filler or fiber, another factor such as fiber orientation, fiber matrix adhesion and all possible mechanisms of fracture, such as fiber pull out and fiber breakage may exist and influence the impact properties. Similarly, in the case of $W-G_c$ relationship, the K_c values for the composites at all fiber loadings decrease significantly with an increase in specimen size. The K_c value for G15 decreases by 15 % from 2.92 MPa $m^{0.5}$ (tensile specimen) to 2.47 MPa $m^{0.5}$ (impact specimen). The similar trend was observed for PP, G30 and G45 composites.

As discussed above, generally, an increase in specimen geometry resulted significant enhancement in W and P while G_c and K_c drop gradually. Hassan *et al.* [5] suggested that one cannot make judgment whether certain formulation of materials improves the impact properties or otherwise just by looking at the values of P and W alone. Comprehensive insight information can be provided by the values of G_c. This implies that, when glass fibers are employed, the thickness effect may be enhanced by the decrease in fiber orientation resulting from the thicker specimens. In injection molding, when molten composites were injected into a thicker mold cavity, the fibers have more room for it to disorientate, allowing the fiber to misalign from the melt flow direction (MFD). Laura *et al*. [32] has also reported that with increase in thickness in injection molded specimen, the fiber orientation will decrease. The decrease in fiber orientation associated with a thicker specimen and a transition in the stress state in the vicinity of the notch are both likely to decrease the fracture energy of the thicker specimens. Additionally, as the thickness of specimen is reduced, more energy will be dissipated as a result of plastic deformation near the specimen surface [33]. Khalid [10] in his study observed a decrement in impact strength when increasing the specimens span length to depth ratio of above 6. This phenomenon was found for both steel and composite specimens tested at room temperature.

Effect of Temperature

Plots of P and W against temperature of T/G30 and I/G30 composites specimen are shown in Figure 7; and their Property Index (PI) values are tabulated in Table 1. The PI values, where the property for the specimen at 25 °C was taken as reference, were calculated using the following general equation:

$$\text{Property Index} = \frac{P}{P_{25^\circ C}} \tag{4}$$

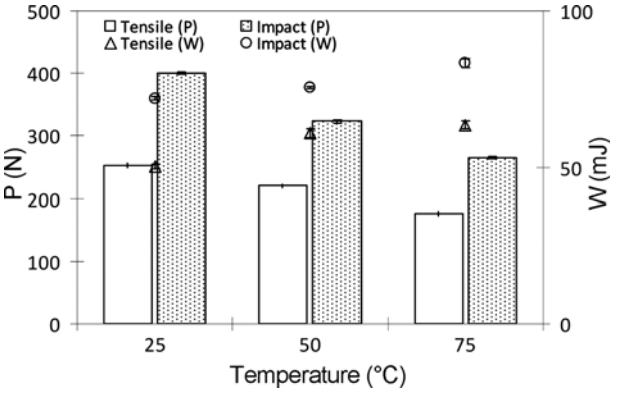

Figure 7. Peak load (P) and fracture energy (W) of PP/G30 composites tested at different temperatures.

Table 1. Property index (PI) of impact properties of glass fiber composites with 30 % W_fGF

Sample	Temperature (°C)	Peak load (P)		Fracture energy (W)		G_c		K_c	
		Value (N)	PI	Value (mJ)	PI	Value (kJ m^{-2})	PI	Value (MPa $m^{-0.5}$)	PI
T/G30	25	253	Ref	50	Ref	2.64	Ref	3.36	Ref
	50	220	0.87	61	1.21	3.17	1.20	2.77	0.82
	75	176	0.69	64	1.26	3.30	1.25	2.18	0.64
I/G30	25	401	Ref	72	Ref	2.22	Ref	2.93	Ref
	50	323	0.81	75	1.05	2.33	1.05	2.36	0.81
	75	265	0.66	83	1.16	2.59	1.17	1.95	0.67

Note: Ref = reference.

where, P_{25^oC} is the respective property of a reference composite at 25 °C, and P is the corresponding property of the composite at different temperatures from which a comparison is to be made.

From Figure 7 and Table 1, it can be seen that P and W are affected by the temperature for both tensile and impact specimens. The P values of T/G30 are reduced from 253 N (25 °C) to 220 N (13 %) and 176 N (31 %), for 50 °C and 75 °C, respectively. The same trend is observed for impact specimen, whereby increase in temperature has lowered the P values of I/G30 from 401 N for 25 °C to 323 N and 265 N, for 50 °C and 75 °C, respectively. For comparison, load versus time curves of T/G30 composite specimens at different temperatures were plotted in Figure 8. As the temperature increases from 25 °C to 75 °C, the composite becomes softer and reduces the load at the fracture point.

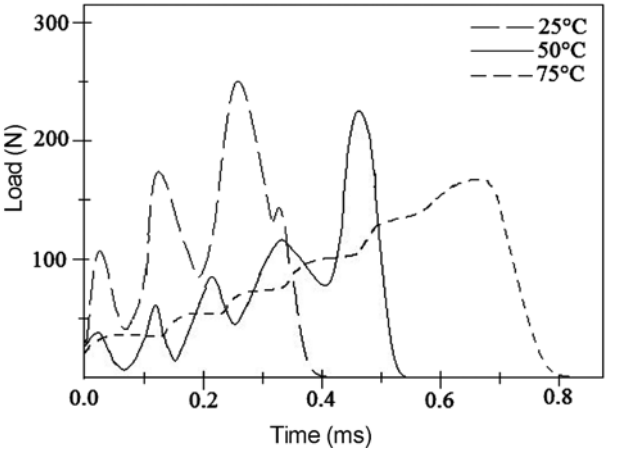

Figure 8. Load-time curves of T/G30 composite specimens tested at different temperatures.

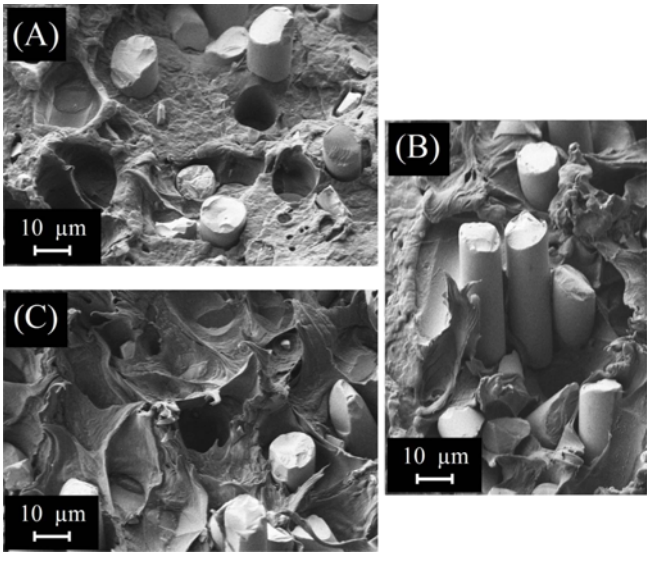

Figure 9. SEM images of impact fractured surfaces of T/G30 at (A) 25 °C, (B) 50 °C, and (C) 75 °C.

The fractured surfaces after impact testing of T/G30 composites at different temperatures were studied by SEM (Figure 9). In the case of composite tested at 25 °C, there is clear evidence of brittle matrix deformation (Figure 9(a)). On the other hand, as temperature is increased (Figures 9(b) and 9(c)), a more ductile fracture surface is observed. It can be noted from Figure 9 that ductility is increased with increase in temperature.

As W is derived from the area under the curve in Figure 8, despite the reduction in P, W of tensile and impact specimens increase with increase in temperature (Figure 7). Increment of temperature from 25 °C to 50 °C and 75 °C further improves W from 50 N to 61 N and 64 N and from 72 N to 75 N and 83 N, for T/G30 and I/G30, respectively. Generally, for all temperatures tested, P and W for impact specimen are higher than those of tensile specimen. As discussed previously, the specimen dimension plays an important role in determination of P and W values of composites.

The G_c of the composite which is directly proportional to the value of W also increases with increasing temperature (Figure 10). The G_c value of T/G30 increases from 2.64 kJ m^{-2} for 25 °C to 3.17 kJ m^{-2} (20 %) and 3.30 kJ m^{-2} (25 %), for 50 °C and 75 °C, respectively. Similar trend has been reported by Khalid [10]. The effect of temperature is less pronounced with impact specimen, as increase in temperature only resulted in increment of about 5 % and 17 % of G_c at 50 °C and 75 °C, respectively, relative to G_c value of I/G30 at 25 °C.

Conversely, K_c of tensile and impact specimens which is related to P value decline with increase in temperature. Increase of temperature from 25 °C to 50 °C and 75 °C further reduce the K_c from 3.36 MPa $m^{-0.5}$ to 2.77 MPa $m^{-0.5}$ and 2.18 MPa $m^{-0.5}$ and from 2.93 MPa $m^{-0.5}$ to 2.36 MPa $m^{-0.5}$ and 1.95 MPa $m^{-0.5}$, for T/G30 and I/G30, respectively. As reported in previous study [34], T_g for PP composite was between 0 °C to 3 °C, at which with temperature higher than this, the matrix will be in the rubbery state, rather the glassy

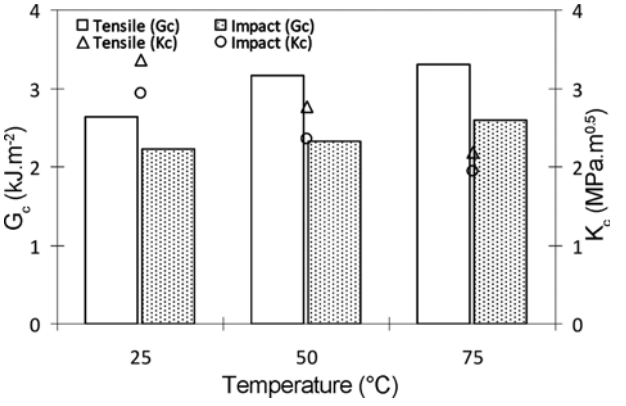

Figure 10. Impact strength (G_c) and fracture toughness (K_c) of PP/G30 composites tested at different temperatures.

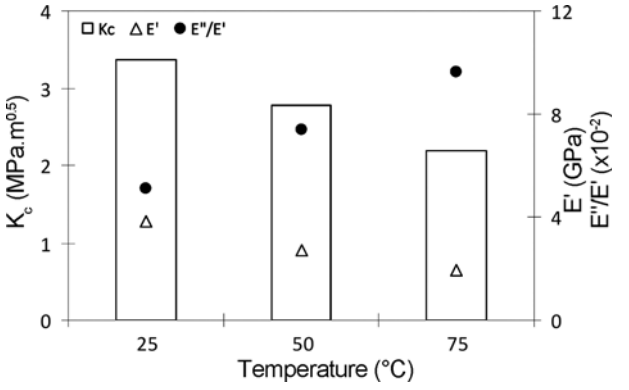

Figure 11. Fracture toughness (K_c), storage modulus (E') and tan delta (E''/E') of T/G30 composites tested at different temperatures.

state. When the temperature is increased further from 25 °C to 75 °C, PP matrix becomes more rubbery and this present the weakest point in fracture toughness. This implies that at temperature above the T_g the strain rate has a strong effect on impact properties. It is noted that at temperatures below T_g, the elongation increases slowly with increasing temperature. At temperatures around T_g, the elongation increases drastically with increasing temperature. When the testing temperature is further increased, the elongation tends to increase. Therefore, the deformation characteristic and bonding strength of the material at different temperature ranges can be employed to explain the phenomenon observed. Alcock *et al.* [35] reported that a large difference in impact performance is observed between composite tested at temperatures below and above T_g value. It is expected since below T_g, semi-crystalline polymers have a much lower strain to failure and hence a lower resistance to crack propagation. This is normally associated with low penetrative impact energy.

This result agrees with those obtained by dynamic-mechanical analysis. The storage modulus (E') and tan δ values at temperature of 25 °C, 50 °C and 75 °C for G30 composite specimen were extracted from Figure 4(a) and (c). For comparison, K_c, E' and tan δ values of T/G30 versus temperature were plotted in Figure 11. Increment of temperature from 25 °C to 50 °C and 75 °C further reduces the E' values from 3.85 GPa to 2.74 GPa (29 %) and 1.94 GPa (50 %). On the other hand, the tan δ values for T/G30 increases from 0.051 at 25 °C to 0.074 (45 %) and 0.096 (88 %) at 50 °C and 75 °C, respectively.

Conclusion

From the FLD characterization, it is found that $\overline{L}_n$ and $\overline{L}_w$ of composites decreased with increase in fiber loading, indicating that more fiber degradation has occurred during processing. Storage modulus of composites is affected by the presence of the glass fiber loading. The $E''_{\max}$ values for the glass fiber composites are higher compared to PP matrix. Incorporation of fibers into the composites has slightly shifted the T_g to lower temperatures. On the other hand, the presence of the glass fiber reduces the magnitude of tan $\delta_{\max}$ values dramatically.

The effects of the specimen size/geometry, glass fiber loading and test temperatures on the impact properties of injection molded polypropylene composites were studied. With respect to increasing in fiber loading, the P values for the composites were increased. For tensile specimen, no significant trend for W was observed with increase in GF content. However, for impact specimen, a sharp decrease in W with the initial incorporation of 15 % W_f of GF loading compared with PP matrix was observed. Further addition of 30 % W_f and 45 % W_f of GF did not produce any significant effect on W.

At the same fiber content, increase in specimen geometry from tensile to impact specimen significantly increased the P and W values, while their corresponding G_c and K_c gradually reduced. By contrast, in the case of PP matrix, the G_c of impact specimen increases by 86 %, relative to tensile specimen.

P and W were affected by the test temperature for both tensile and impact specimens. Despite the reduction in P, W of the tensile and impact specimens increased with increase in temperature. The G_c of the composite which is directly proportional to the value of W also increased with increasing temperature. Conversely, K_c of tensile and impact specimens which is related to P value declined with increase in temperature.

Finally, it can be concluded that impact properties such as P, W, G_c and K_c are very much dependent on the testing conditions such as specimen size/geometry, glass fiber loading and test temperatures, etc. Direct property comparison between one data and the other cannot be made without the knowledge of the test details.

List of abbreviations

3-PB: three point bending
a: notch depth (or crack length)
B: width of specimen
D: depth of specimen
a/D: notch-to-depth ratio
DMA: dynamic mechanical analysis
E': storage modulus
E'': loss modulus
$E''_{25^\circ C}$: magnitude of E'' at 25 °C
$E''_{\max}$: magnitude of E'' at $T_\alpha^{E''}$
FLD: fiber length distribution
FRP: fiber-reinforced polymer
G_c: critical strain energy release rate
GF: glass fiber
GFRP: glass fiber reinforced polymer
K_c: critical stress intensity factor
LEFM: linear elastic fracture mechanics

$\bar{L}_n$: number average fiber length
$\bar{L}_w$: weight average fiber length
MFD: melt flow direction
P: peak load
P_{25^oC} : respective property of a reference composite at 25 °C
PI: property index
PP: polypropylene
S: span of specimen
SEM: scanning electron microscopy
SEN: single edge notch
tan δ: tan delta (loss tangent)
tan δ_{max}: magnitude of tan δ at T_g
T_g: glass transition temperature
T_α: peak at maximum value of tan δ in α-transition (T_g)
$T_\alpha^{E''}$: temperature at the maximum value of E'' in the α-transition region
W: fracture energy
W_f: fiber weight fraction
Y: geometry correction factor
Φ: correction factor
σ: fracture stress

Acknowledgements

The authors wish to thank the University of Malaya who supported the work reported in this paper with grant numbers PPP (PS230-2008B) and FRGS (FP021-2013A).

References

1. J. Josef in "Impact Behavior of Polypropylene and its Blends and Composites" (G. K. Harutun Ed.), Handbook of Polypropylene and Polypropylene Composites, 2nd ed., p.170, New York, Marcel Dekker Inc., 2003.
2. A. A. M. Badawy, *Ain Shams Eng. J*., **3**, 105 (2012).
3. ASTM Standard E-23, Standard Test Method for Notched Bar Impact Testing of Metallic Materials, ASTM International, West Coshoshocken, PA, DOI 10.1520/E0023-07AE01, www.astm.org.
4. M. O. W. Richardson and M. J. Wisheart, *Composites,* **27**, 1123 (1996).
5. A. Hassan, A. A. Hassan, and M. I. Mohd Rafiq, *J. Reinf. Plast. Compos.,* **30**, 889 (2011).
6. E. Lucon, *Inter. J. Fracture.,* **153**, 1 (2008).
7. T. A. Siewert and M. P. Manahan, Pendulum Impact Testing: A Century of Progress, ASTM International, 2000.
8. R. K. Mittal and M. S. Jafri, *Composites,* **26**, 877 (1995).
9. J. L. Thomason, *Compos. Part A-Appl. S.*, **40**, 114 (2009).
10. A. A. Khalid, *Mater. Des.,* **27**, 499 (2006).
11. J. L. Thomason and M. A. Vlug, *Compos. Part A-Appl. S.*, **28A**, 277 (1997).
12. ASTM Standard D-638, Standard Test Method for Tensile Properties of Plastics, ASTM International, West Coshoshocken, PA, 2003, DOI 10.1520/D0638-03, www.astm.org.
13. A. Hassan, N. M. Salleh, R. Yahya, and M. R. K. Sheikh, *J. Reinf. Plast. Compos.,* **30**, 488 (2011).
14. J. Denault, T. Vu-Khanh, and B. Foster, *Polym. Compos.,* **10**, 313 (1989).
15. A. Hassan, R. Yahya, A. H. Yahaya, A. R. M. Tahir, and P. R. Hornsby, *J. Reinf. Plast. Compos.,* **23**, 969 (2004).
16. J. Preston in "Polyamides, Aromatic" (H. F. Mark, N. M. Bikales, C. G. Overberger and G. Menges Eds.), Encyclopedia of Polymer Science and Engineering, 2nd ed., Vol. 11, p.381, New York, John Wiley and Sons, 1988.
17. J. L. Thomason, *Polym. Compos.,* **11**, 105 (1990).
18. A. Hassan, A. R. Normasmira, and R. Yahya, *Fiber. Polym.,* **13**, 899 (2012).
19. ASTM Standard D-790, Standard Test Methods for Flexural Properties of Unreinforced and Reinforced Plastics and Electrical Insulating Materials, ASTM International, West Coshoshocken, PA, 2010, DOI 10.1520/D0790-10, www.astm.org.
20. A. K. Saha, S. Das, D. Bhatta, and B. C. Mitra, *J. Appl. Polym. Sci.,* **71**, 1505 (1999).
21. S. K. Nayak and S. Mohanty, *J. Reinf. Plast. Compos.,* **29**, 1551 (2010).
22. J. George, S. S. Bhagawan, and S. Thomas, *J. Therm. Anal. Calorim.,* **47**, 1121 (1996).
23. S. Mandal and S. Alam, *J. Appl. Polym. Sci.,* **125**, E382 (2012).
24. S. Mohanty, S. K. Verma, and S. K. Nayak, *Compos. Sci. Technol.,* **66**, 538 (2006).
25. A. R. Normasmira, A. Hassan, R. Yahya, R. A. Lafia-Araga, and P. R. Hornsby, *J. Reinf. Plast. Compos.,* **31**, 1247 (2012).
26. M. A. López-Manchado, J. Biagiotti, and J. M. Kenny, *J. Thermoplast. Compos. Mater.,* **15**, 337 (2002).
27. J. M. Crosby and T. R. Drye, *J. Reinf. Plast. Compos.,* **6**, 162 (1987).
28. N. J. Lee and J. Jang, *Compos. Part A-Appl. S.*, **30**, 815 (1999).
29. V. B. Gupta, R. K. Mittal, P. K. Sharma, G. Mennig, and J. Wolters, *Polym. Compos.,* **10**, 16 (1989).
30. J. K. Wells and P. W. R. Beaumont, *J. Mater. Sci.,* **20**, 1275 (1985).
31. V. B. Gupta, R. K. Mittal, and M. Goel, *Compos. Sci. Technol.,* **37**, 353 (1990).
32. D. M. Laura, H. Keskkula, J. W. Barlow, and D. R. Paul, *Polymer,* **41**, 7165 (2000).
33. G. Caprino and V. Lopresto, *Compos. Sci. Technol.,* **61**, 65 (2001).
34. A. Hassan, A. R. Normasmira, and R. Yahya, *J. Reinf. Plast. Compos.,* **30**, 1223 (2011).
35. B. Alcock, N. O. Cabrera, N. M. Barkoula, Z. Wang, and T. Peijs, *Compos. Part B-Eng.,* **39**, 537 (2008).